

HIGH DYNAMIC RANGE POINTING MECHANISM

Eric Lorigny*, Gabriel Pont* et Vincent Albouys**

Centre National d'Etudes Spatiales

*Mechanism Department, **Structures and Mechanics Department

BPI 1416; 18, avenue Edouard Belin; 31401 Toulouse Cedex 04

Telephone: 33 5 61 28 27 15/ Fax: 33 5 61 28 29 85

E-mail: Eric.Lorigny@cnes.fr/Gabriel.Pont@cnes.fr/Vincent.Albouys@cnes.fr

ABSTRACT

Earth observation satellites require a high availability for imaging that means a quick angular displacement of the field of view and a high stability of the line of sight just after moving. This quick displacement should not disturb the satellite attitude control.

When a cable wrap needs to be implemented through the rotating joint, a high driving torque is also mandatory to guarantee the accuracy of the actuation. With these objectives, CNES has developed a mechanism prototype able to fulfil these requirements. This paper presents the mechanism design and the test results associated.

1. INTRODUCTION

For the new generation of earth observation satellite, CNES has developed a concept of mini-satellite based on a PROTEUS platform. This new earth observation satellite, called 3S, is designed with two degrees of freedom instrument. One axis is the north/south scanning, done by a mechanism driving a steering mirror, the second one is the east/west scanning, done by a mechanism driving the whole instrument. The movement of the whole instrument is mandatory to ensure the geometrical properties of the image. This second mechanism, called MAMOC, is the subject of this paper.

2. REQUIREMENTS

The main performance requirements are summarised in the following table:

Parameter	Requirement
Inertia of the whole instrument	3,4 kg.m ²
Instrument weight	90 kg
Angular stroke	+/-45°
Number of cycles on 5 years	> 300 000
Stroke time for 60°	< 10 seconds
Stabilisation time	< 4 seconds
Pointing accuracy	< 100 µrad
Localisation accuracy	< 15 µrad
Position stability over 2 ms	< 0,5 µrad
Speed oscillation	< 50 µrad/s
Reaction torque transmitted to the satellite platform	< 0,1 Nm
Power consumption when stopped	< 0,5 watt

Table 1

With all the requirements, the instrument needs also 110 wires of 24 AWG shielded, twisted and 25 coaxials in order to provide the instrument data transfer, detection, motor supply of the steering mechanism, thermal control, ...

3. MAMOC DESIGN DESCRIPTION

The MAMOC (Autocompensation Mechanism of the Kinetic MOMentum) must have a high torsional and bending stiffness to ensure the first bending mode above 10 Hz with the instrument and a torsional mode as high as possible (objective > 15 Hz).

The MAMOC mechanism is basically composed of:

- ? a Harmonic Drive gear reducer
- ? a high speed stepper motor
- ? an optical encoder

All these elements are integrated in a MGRA 42 cartridge from SAGEM. This cartridge includes two ball bearings pairs, one X mounted on the input stage, and the others O mounted on the output stage.



Figure 1: The MAMOC cartridge

The two following more elements are necessary to achieve the mission:

- ? a wires reel for the instrument operation
- ? a locking device for the launch vibrations

Its main function is to ensure the displacement with a compensation of the kinetic momentum. To achieve this performance, the input shaft inertia is equal to the

instrument inertia divided by the gear ratio of the reducer (see paragraph 5).

3.1 Description of the Harmonic Drive reducer

An Harmonic Drive reducer is used because its rather good torsional stiffness, long life expectancy with wet lubrication, excellent positioning accuracy, and high torque capability. Moreover, the input revolution sign is the opposite of the output one, allowing a kinetic momentum compensation (see paragraph 5).

With the high numbers of wires to reel and the high dynamic performance required, we have a compromise to do between the torque and the speed.

To achieve a good auto compensation of the kinetic momentum, we need to have a high gear ratio to limit the added input inertia (see paragraph 5).

The chosen gear ratio for the Harmonic Drive is 160.

The output angular stiffness measured is 45 000 Nm/rad.

3.2 High speeds stepper motor design

With a high gear ratio, the motor needs to turn at a quite high speed. With a specification of 60° in 10 seconds for instrument rotation, the motor speed required is about $1500^\circ/\text{s}$. And to ensure a high stability with no power consumption, the highest torsional stiffness is needed.

The brushless motor needs a closed control loop and it does not present torsional stiffness without supply voltage.

So, the stepper motor solution was considered as the best choice but it presents difficulty to rotate at high speeds.

SAGEM developed a stepper motor able to reach more than $3000^\circ/\text{s}$ under 28 volts with a $3,5 \text{ kg.m}^2$ inertia load. To achieve this performance, the stator is laminated, and the wiring resistance is reduced to less than 5Ω . The constant torque is $0,6 \text{ Nm/A}$.

3.3 Position sensor

A Codechamp 21 bits optical encoder is used for the measurement of the displacement : the resolution is $3 \mu\text{rad}$ and the precision on 360° is better than $15 \mu\text{rad}$.

This encoder is linked to the output shaft.

3.4 The wires reel

The 110 wires of AWG24 and the 25 coaxials are grouped into three cable bundles. The 45 wires of each bundle are sewed together. Some PTFE strips are installed each 20 cms to stiffen the cable bundle.

The wires reel was tested alone in order to measure its main characteristics. (see fig.2).



Figure 2: The wires reel in the bench test

The measured induced torque hysteresis is the following:

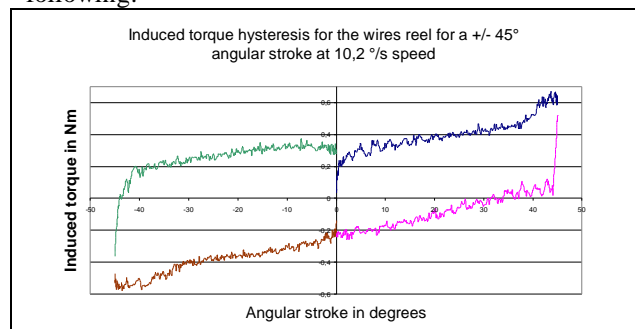


Figure 3: Induced torque in the wires reel

3.5 The locking device

To limit the impact of launch vibrations on the ball bearings of the cartridge, a locking device has been added on the 3S instrument. In the launch attitude, a $0,6 \text{ mm}$ deflection is imposed on 3 flex blades, so that the ball bearings are not overloaded during the take off. The test on the bench has demonstrated that the load level to comply with vibrations is about 1500 N / blade . This level is compatible with the capacities of the locking devices (AMF).

4. DESCRIPTION OF THE TEST BENCH

A mock-up, inertia, centre of gravity, weight, three first modes representative, was built to simulate the structural behaviour of the instrument.

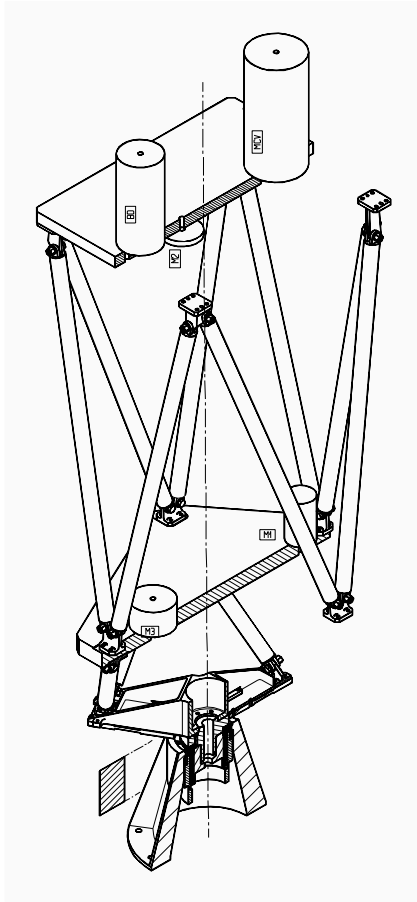


Fig 4: lest instrument

The flex blades are flight representatives to simulate the locking device. Three threaded rods are used to preload the instrument.

4.1 sensors

The optical encoder, included in the mechanism, measures the output angular displacement. An additional high sensitive angular sensor (Systron Donner) measures the stability with a 10 μ rad range.

A piezoelectric torquemeter measures the reaction torque induced on the satellite during displacement.

4.2 software acquisition

The "Labview" software is used for the acquisition of the optical encoder, the angular sensor and the piezoelectric torquemeter.

The motor driving is performed by a specific electronic via Labview software.

In figure 5, the first quarter (in clockwise sense) represents the output encoder turlututu, second one is either the torquemeter or the angular sensor indication, third one is the FFT of the second quarter signal. The last quarter is the input command (initial speed, final speed, number of microsteps/step, angular stroke,

acceleration duration, acquisition frequency (? 1000 Hz) and acquisition duration).



Figure 5: software acquisition screen

In all of the tests, the stepper motor is driven at 64 microsteps/step.

5 THE AUTOCOMPENSATION PRINCIPLE

When an inertia (I_1) is moved at a speed of ω_1 , the kinetic momentum is completely transmitted to the satellite and the AOCS wheels must deliver a negative kinetic momentum feedback.

The kinetic momentum compensation needs two mechanisms excepted if as MAMOC, the input shaft rotates in the opposite sense of the output. In this case, and if the input shaft inertia (I_2), is equal to the instrument inertia divided by the gear ratio (R).

In this application, $I_1=3,4 \text{ kg.m}^2$, and $R=160$, so I_2 must be equal to $2,125 \cdot 10^{-2} \text{ kg.m}^2$.

In fact, the reaction wheel is included into MAMOC in the input shaft. The main drawback is that the stepper motor needs more torque to accelerate this additional inertia.

6. TEST RESULTS

6.1 Modal analysis

A modal analysis has been performed to confirm that the first bending mode value was about [10;12] Hz and the first torsion mode value $> 15 \text{ Hz}$.

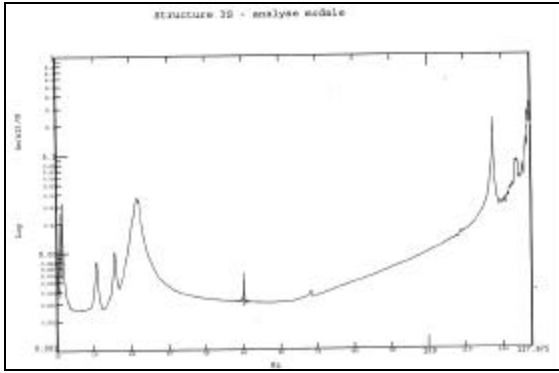


Figure 6: analysis modal curve

An electrodynamic exciter and 4 accelerometers have allowed to measure the following values:
 $f_1 = 10.7 \text{ Hz}$, $f_2 = 15.5 \text{ Hz}$: bending modes,
 $f_3 = 20.6 \text{ Hz}$, torsion mode that confirm that the torsion stiffness of the cartridge is about 5.10^4 Nm/rad .

6.2 Reaction torque on platform

Two series of tests were done one with the compensation inertia and one without.

In both cases, the torque transmitted ($T_{reaction}$) to the satellite platform is:

$$T_{reaction} = (I_{instrument} - R * I_{input}) * w'_{output}$$

Where w'_{output} is the output acceleration in rad/s^2 .
 With in the first case, an input inertia equal to $0,9 \cdot 10^{-4} \text{ kg.m}^2$, and in the second one $I_{input} = 2,125 \cdot 10^{-2} \text{ kg.m}^2$.

The rate torque is the same with or without inertia compensation and looks like this:

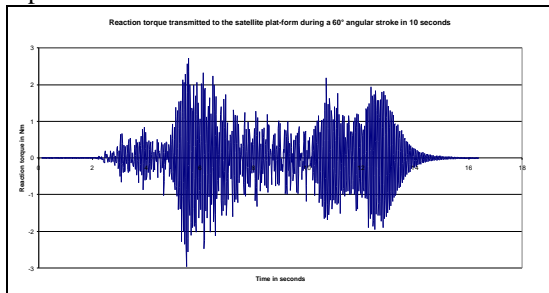


Figure 7: reaction torque transmitted

The mean value is quasi null with the compensation inertia whereas the mean value is equal to $(I_{instrument} - R * I_{input}) * w'_{output}$ without.

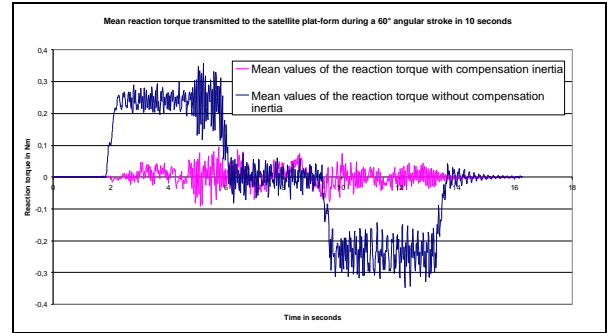


Figure 8: Mean reaction torque

The discrete values are similar because the motor driving excites the torsional mode and the speed oscillation adds dynamic reaction torque due to the acceleration at high frequency (around 18 Hz).

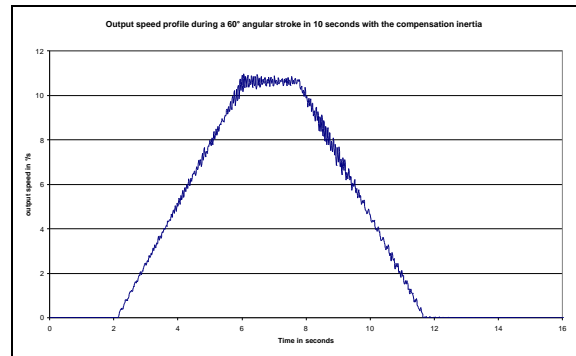


Figure 9: output speed profile

In the speed profile, the oscillation can reach $0,8^\circ/\text{s}$ in $1/36 \text{ s}$, so a reaction torque peak of $3,4 \text{ Nm}$.

These oscillations have few influences on the AOCS of the satellite. The drawing below shows the depointing of the PROTEUS platform ($I=360 \text{ kg.m}^2$), with a 60° angular stroke in 10 seconds with the compensation inertia:

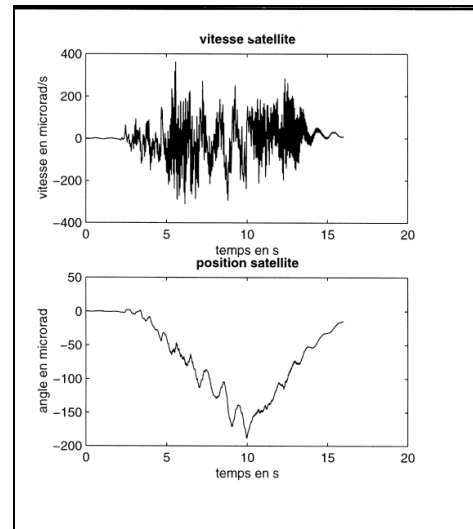


Figure 10: platform responses

The platform needs a torque of 0,02 Nm to rebalance itself., and the maximal speed peak is 400 $\mu\text{rad/s}$. So, with a complete compensation of the kinetic momentum, the reaction torque is null which is quite a major challenge for the AOCS purpose.

6.3 Angular stability

The instrument is placed on a marble. The noise of the angular sensor, when the instrument is at rest, corresponds to a sine of +/- 0,2 μrad (peak to peak) at 10 Hz that gives a speed noise of 8 $\mu\text{rad/s}$ with no supply voltage

After a displacement, this sensor can give us the time to reach the stability requirement of 50 $\mu\text{rad/s}$.

The test results showed that neither the angular stroke nor the speed reached, have impacts on the stabilisation time. The time between reaching position and decreasing speed oscillation below 50 $\mu\text{rad/s}$ is about 2 seconds.

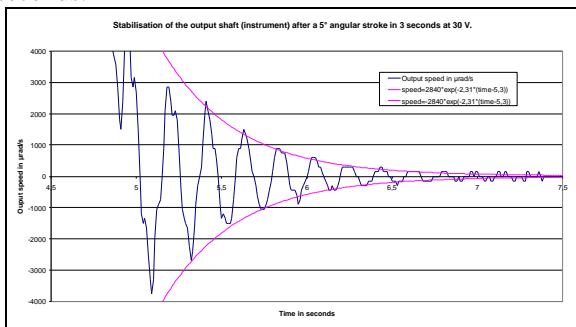


Figure 11: instrument stabilisation

6.4 Dynamic capacities

All the dynamic tests are done at 64-microstep/electrical step, and the motor is a 360 mechanical step/revolution. The current limitation is 0,5 A.

Criteria in the input shaft/supply voltage	30 V	90 V
Max. speed without load in $^\circ/\text{s}$		6 565
Max. accel. without load in $^\circ/\text{s}^2$		29 540
Max. speed with $2,2 \cdot 10^{-4} \text{ kg.m}^2$ in $^\circ/\text{s}$	3 800	4 478
Max. accel. with $2,2 \cdot 10^{-4} \text{ kg.m}^2$ in $^\circ/\text{s}^2$	12 700	21 570
Max. speed with $2,15 \cdot 10^{-2} \text{ kg.m}^2$ in $^\circ/\text{s}$	1 500	1 700
Max. accel. with $2,15 \cdot 10^{-2} \text{ kg.m}^2$ in $^\circ/\text{s}^2$	448	528

Table 2

The inertia calculated is the inertia reported to the input shaft. Without load means only HD inertia + rotor inertia ($0,9 \cdot 10^{-4} \text{ kg.m}^2$). The $2,2 \cdot 10^{-4} \text{ kg.m}^2$ is the instrument inertia ($3,4 \text{ kg.m}^2$) reported on the input shaft (divided by the square gear ratio).

The $2,15 \cdot 10^{-2} \text{ kg.m}^2$ inertia is the last case added with the compensation inertia ($2,125 \cdot 10^{-2} \text{ kg.m}^2$).

With the compensation inertia, the inertia seen by the motor is multiplied by approximately one hundred. So, the acceleration performance decreases a lot and now the supply voltage has nearly no influence on the dynamic performances.

The maximal speed cannot be reached with the compensation inertia because the software has a maximal acceleration duration of 4 seconds. So with the acceleration limitation (due to the high inertia) and the duration limitation (due to the software), the maximal speed was limited.

6.5 Pointing precision

The MAMOC mechanism is put in an other test bench to measure the influence of an external torque on the pointing precision.

In this new test bench, the external torque is applied by an other motoreducer directly on the output inertia.

The pointing precision is depending mainly of two factors: the external torque and the rotation sense.

The pointing precision does not depend on the angular stroke.

The secondary factors are the inertia and physical position (for example: the pointing precision at 11° is better than the pointing precision at 23° , see figure 12).

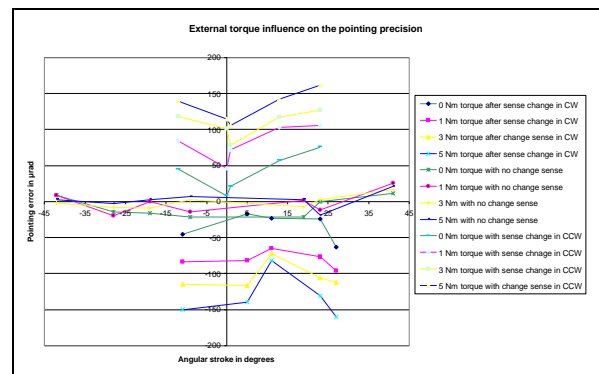


Figure 12: pointing precision

The following table summarises the precision results in μrad :

Precision/ext. torque	0 Nm	1 Nm	3 Nm	5 Nm
Max error	76	106	127	162
Min error	-63	-96	-117	-150
Mean error	27,7	52,8	65,4	74,6

Table 3

The external torque increases the pointing accuracy due to the angular stiffness of the Harmonic Drive.

$$J_{total_error} = J_{error_0Nm} + \frac{T_{external_torque}}{K_{HD_angular_stiffness}}$$

With a 45 000 Nm/rad stiffness, the error increases up to 22 $\mu\text{rad/Nm}$.

The wires reel can reach 0,6 Nm (see figure 2), so the pointing accuracy is better than +/- 100 μrad in laboratory conditions.

6.6 Power consumption

The motor has two coils. The coils consumes:

$$I_{coil_1} = 0,5 * \sqrt{2} * \sin \mathbf{v}t \text{ under 30 volts.}$$

$$\text{and } I_{coil_2} = 0,5 * \sqrt{2} * \cos \mathbf{v}t \text{ under 30 volts.}$$

So the maximum power consumption is 30 watts.

This power is consumed only during a displacement (maximum time of 10 seconds). After this, the instrument takes the picture while the motor is off and waiting for the next command. With 300 000 cycles during 5 years, the average power consumption is lower than 0,5 watts/hour.

With a motor resistance lower than 5 Ω , the maximal thermal dissipation is the motor is lower than 2,5 watts and the average thermal dissipation lower than 0,05 watts/hour during the instrument life.

A test was done at 0,3 A (18 W) instead of 0,5 in the two coils, but the 60° angular stroke was ran over in 17s instead of 11s.

7 CONCLUSIONS AND PERSPECTIVES

MAMOC is able to:

- Achieve 60° angular stroke in less than 13 seconds (instrument and satellite stabilisation included); and 5° in 5 seconds.
- Reach a pointing position with a precision better than +/- 55 μ rad at 1 s with an external torque of 0,6 Nm.
- Deliver an output torque greater than 30 Nm under 30 volts.
- Roll 110 wires of AWG 24 and 25 coaxials for the instrument operations.
- Stabilise the instrument with no power supply with an angular stiffness of 50 000 Nm/rad (displacement when an external torque is greater than 8 Nm).
- Have a transverse shaft stiffness of 1,2 10^6 Nm/rad, and a linear axial and radial stiffness of 2,5 10^8 N/m.
- Consume 30 watts only during a displacement.
- Have a fully compensation of induced reaction torque whatever the acceleration requested.

This mechanism can be used whenever an inertia has to be moved at high speed with high precision, with an easy compensation of the kinetic momentum.

This mechanism is robust to external perturbations.

The weight of this mechanism is depending of the inertia to compensate and required stiffness (between 3,5 and 6 kg).

This mechanism is patented by CNES.



Figure 13: The configuration tested